PHYSICAL REVIEW A VOLUME 6, NUMBER 1 JULY 1972

Electron Transmission Spectroscopy: Core-Excited Resonances in Diatomic Molecules*

L. Sanche and G. J. Schulz
Department of Engineering and Applied Science,
Mason Laboratory, Yale University, New Haven, Connecticut 06520
(Received 18 January 1972)

A high-resolution and high-sensitivity electron transmission spectrometer is used to study sharp structures in the total scattering cross section of H_2, D_2, O_2, NO, N_2, and CO. Many new resonances are found, some of which form bands which consist of progressions of negative-ion vibronic states. The existence of bands makes the identification of temporary negative-ion states easier, since the spacing and the magnitudes of the structure can be compared with the appropriate parameters of various positive-ion cores. The most prominent features observed consist of two Rydberg electrons attached to a particular positive-ion core.

I. INTRODUCTION

Electron transmission spectroscopy has proved to be of great value for the study of compound-state formation in electron-atom[1] and electron-molecule scattering.[2,3] We have recently reported[4] many new resonances in the total scattering cross sections of the rare gases using an electron transmission spectrometer of high resolution and high sensitivity. In this paper we report electron transmission spectra for H_2, D_2, N_2, CO, O_2, and NO which were obtained in the same apparatus.

In the past decade a considerable number of fine structures have been observed in the total scattering cross sections of diatomic molecules. Most of these structures were identified as resonances,[3] which can be classified into two major categories,[5] namely, (i) "single-particle" or "shape" resonances in which the incident electron with finite angular momentum is temporarily captured in the ground electronic state of the molecule. The effective potential barrier is created by the centrifugal, polarization, and exchange forces, and (ii) "core-excited" resonances which consist of an electron temporarily bound to an excited state of the molecule.

Shape resonances associated with the ground electronic state lie 0–3 eV above the ground state of the molecule. Their existence is well established in molecules, and their lifetimes vary from 10^{-10} sec for[6] O_2 to about 10^{-15} sec in the case of[7] H_2. Shape resonances in diatomic molecules have been studied extensively and therefore shall not be the object of the present investigation. In atoms, no low-lying shape resonances have been conclusively observed to date.

Core-excited resonances can be divided into two further subcategories[5]: (i) type I which appear below their respective excitation thresholds and (ii) type II which occur slightly above the thresholds of excited target states. We shall refer to type-I resonances simply as core-excited resonances and to type II as core-excited shape resonances, since in this resonant process the electron trapping depends on the shape of the potential well induced by the angular momentum of the electron and the excitation and polarization of the target. Core-excited shape resonances are not expected in the s wave, but they have been observed[8] in the p and d waves. In atoms, core-excited shape resonances are often broader (0.1–0.5 eV) than core-excited resonances. The latter have natural widths of the order of 1–10 meV. In atoms, most excited states have core-excited resonances associated with them and each of these resonances necessarily consists of two electrons trapped in the field of a singly charged ion core.

In molecules, a core-excited resonance may consist, in principle, of an electron temporarily bound to either a valence or a Rydberg excited state. However, when calculations[9] are made on the binding nature of the additional electron, it is found that only Rydberg excited states have a positive electron affinity for a fixed internuclear separation in the Franck-Condon region. Therefore, we expect to find sharp resonances slightly below the excitation thresholds only for Rydberg excited states. In this case, the temporary negative-ion complex consists of two Rydberg electrons trapped in the field of a positive-ion core, i.e., the grandparent state. The parent (or parents) consists of a single Rydberg electron bound by the field of the same ionic core.

Core-excited resonances have lifetimes (10^{-12}–10^{-13} sec) which are long compared to the vibrational period of a molecule and therefore can give rise to bands, each of which consists of a progression of vibrational levels. Since the two Rydberg electrons trapped by the ion core are nonbonding, we expect the negative ion and its grandparent positive-ion core to have similar vibrational spacings and Franck-Condon probabilities. We can thus compare the vibrational spacings and Franck-Condon probabilities for a given band of negative-ion vi-

bronic states with the corresponding values for the many possible positive-ion states of a molecule in order to identify the parentage and electron affinity of the band under investigation. When the width of each member of a progression is independent of the vibrational energy, the Franck-Condon probabilities for Rydberg negative-ion formation can be obtained by measuring the relative magnitude of each vibrational member of a progression in the transmission spectra, assuming that in the experiment the intensity of the primary electron beam and its resolution are kept constant.

In some cases, progressions may overlap, making their identification difficult. In other instances, the width of a core-excited resonance may change due to the opening of a new channel of decay. If the resonance decays completely into such a new channel which happens to be a repulsive state of the negative-ion system, the vibrational progression may stop abruptly after a certain vibrational level. In this case, the progression may completely or partially predissociate depending on the energy position of the repulsive state. This situation may arise from an avoided crossing between two states of the same symmetry.

Certain negative-ion states are probably not seen at all in transmission experiments because their natural width is too large or because their Franck-Condon probabilities for excitation from the ground state are too small.

II. EXPERIMENT

Structure in the total scattering cross sections of diatomic molecules is studied by measuring the unscattered current transmitted through a gas-filled collision chamber. We measure directly the derivative of this transmitted current.

The apparatus is a high-resolution and high-sensitivity electron transmission spectrometer which has recently been described[4] in detail. Figure 1 shows a diagram of the apparatus. Electrons emitted from a thoria-coated iridium filament F are aligned by an axial magnetic field B of about 100 G and traverse a trochoidal monochromator[10] to produce an electron beam of about 5×10^{-9} A with an energy spread (full width at half-maximum) between 20 and 30 meV. The electron beam which leaves the monochromator is accelerated into a collision chamber where its intensity is attenuated by the presence of the gas under investigation. Only the unscattered portion of the electron beam is measured at the collector C, since scattered electrons have their velocity vector reoriented and are unable to overcome the potential barrier provided by the two retarding electrodes R.

In order to measure the derivative of the transmitted current, we apply a sine wave of variable amplitude (5–50 mV) between the collision chamber and an insulated cylinder M which is inserted inside the collision chamber. The resulting modulation on the transmitted current measured at electrode C is amplified and then measured in phase with the modulation signal by means of a phase-sensitive (lock-in) detector. During each sweep of the electron accelerating voltage, the modulation signal is kept constant and thus the output signal from the phase-sensitive detector is directly proportional to the derivative of the transmitted current.

The ac component of the transmitted current is approximately given by

$$\Delta I \simeq - I_0 L N \frac{dQ_t}{dE}\, e^{-NQ_tL} ,$$

where I_0 is the current entering the collision chamber, $Q_t(E)$ is the total scattering cross section for electrons of energy E, L is the path length, and N is the gas density. For small structures in the transmitted current, the measured modulation on the transmitted current ΔI is to a first approximation directly proportional to (dQ_t/dE). The many advantages of this method for observing resonances have been discussed previously in our work[4] on rare-gas atoms.

III. INTRODUCTION TO RESULTS

In the following sections we discuss derivative electron transmission spectra for H_2, D_2, CO, N_2, NO, and O_2. Each spectrum exhibits many resonances in the total electron impact cross section. Some of the structures are isolated and some form bands. The parentage and grandparentage of the resonances is deduced from the spacings and the amplitudes of the structures.

The line shape of a resonance possesses two or

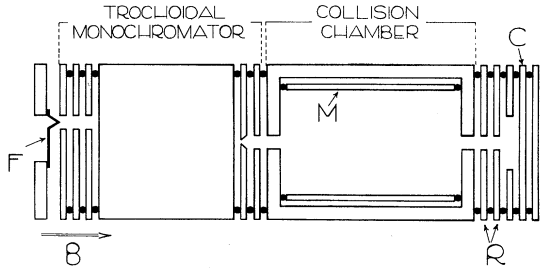

FIG. 1. Schematic diagram of electron transmission spectrometer. Electrons are emitted from the filament F and aligned by a magnetic field B and energy selected by a trochoidal monochromator. They enter the collision chamber where a small modulating signal (5–50 meV, 730 Hz) is applied to M and the transmitted current is detected synchronously at the collector C. The retarding electrodes R provide a potential barrier for scattered electrons.

three inflection points, depending on the phase shift of the potential scattering. When the phase shift for potential scattering is $\frac{1}{2}n\pi$, two inflection points result, and the derivative exhibits a single maximum and a single minimum. When the phase shift for potential scattering is removed from $\frac{1}{2}n\pi$, the resonance shape shows three inflection points and the derivative has two minima and one maximum, or two maxima and one minimum. However, only a single maximum and a single minimum may be visible when the phase shift for potential scattering is not far removed from $\frac{1}{2}n\pi$, because the slope of the resonance profile is large only at two points. When the phase shift for potential scattering is far removed from $\frac{1}{2}n\pi$, the slope is large only at a single inflection point and thus the derivative may have only a single well-pronounced dip or peak. The subsidiary structures in the wings of the line are often not visible since they may be hidden by other structures.

The structures observed in the present work are identified using the guidelines given above. Since the position of maximum slope in a resonance profile lies close to the center of the resonance, the most pronounced maximum (or minimum) is chosen as the energy of the resonance. Band assignments are made whenever a regular progression of peaks or dips occurs.

All the energy scales in this work are calibrated by referring the observed structures to the 19.34 ± 0.02-eV resonance in helium and the 11.10 ± 0.03-eV resonance in argon.[4] This is done by admixing small amounts of He or Ar to the gas under investigation. Our energy scales are accurate within 30 meV relative to the helium or argon resonances and possess an *absolute* error of ± 0.05 eV, unless otherwise stated.

Most of the resonances observed in this work produce variations in the transmitted current (for $NQ_t L \simeq 1$) between 1 and 0.01%. All the electron transmission curves presented are direct X-Y plots of the derivative of the transmitted current vs the electron impact energy.

IV. RESULTS IN H_2 AND D_2

The region between 11 and 16 eV in H_2 and D_2 has been investigated intensively by several groups who find many structures in the elastic and inelastic electron-impact cross sections. In this section we discuss the structure we observe in the total electron scattering cross section of H_2 and D_2 within the framework of the available information on the formation and decay of the H_2^- and D_2^- compound states. Table I shows a review of the recent experimental results including those of the present experiment. The bands are designated "*a*" to "*g*," and the results of individual authors are listed on subsequent lines. Also given are the name used by each author for a particular band, the channel of observation, and the energy of the first vibrational level of each band. Below we discuss each band in detail.

TABLE I. Summary of experimental data on H_2^-. The symbol × indicates that band "*b*" is observable only in the high vibrational states ($v > 8$) of the $^1\Sigma_g^+$ state and thus it is very difficult, maybe impossible, to observe in transmission experiments.

Possible equivalence[a]	←		→		←	→	
Band designation	"*a*"	"*b*"	"*c*"	"*d*"	"*e*"	"*f*"	"*g*"
Kuyatt *et al.* (Ref. 12) (transmission)	"strong" 11.28	×	"weak" 11.46				
Comer and Read[b]	$X\,^1\Sigma_g^+(v)$ 11.30	$X\,^1\Sigma_g^+$ ($v>8$) 11.11	$X\,^1\Sigma_g^+(v)$ 11.40				
Weingartshofer *et al.*[c]	"series I" 11.30			"series I" $B\,^1\Sigma_u^+$ 11.30	"series II" $B\,^1\Sigma_u^+$ 11.50	$C\,^1\Pi_u$ 13.63	
Sanche and Schulz[d] (transmission)	11.32	×	11.43			13.66	15.09
Width, Γ (eV)	0.045 (H_2)[b]	0.03[b]				0.08[c]	
Symmetry	$^2\Sigma_g^+$	$^2\Sigma_g^+$	$^2\Sigma_g^+$; $^2\Pi_u$	$^2\Pi_g$(?)		$^2\Sigma_g^+$	
Observed in	H_2, HD, D_2	H_2	H_2, HD, D_2	H_2	H_2	H_2, D_2	H_2, D_2

[a]The arrows indicate that band "*a*" could be identical to band "*d*" and that band "*c*" may be identical to band "*e*".
[b]Reference 18; the decay channel for each band is given.
[c]Reference 15; the decay channel for each band is given.
[d]Present experiment.

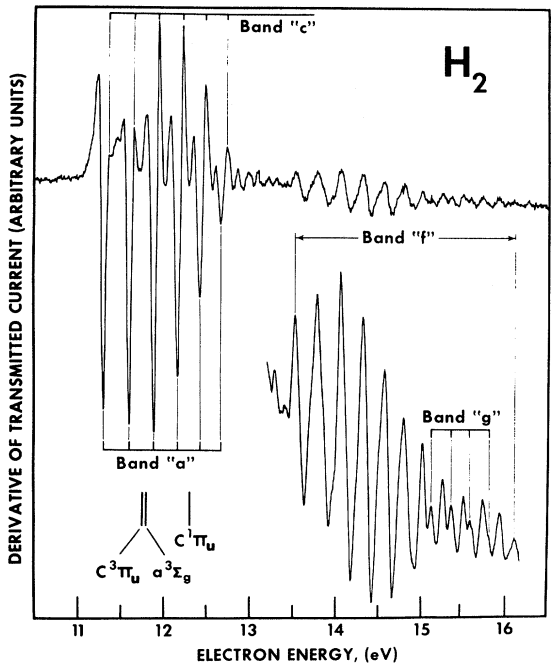

FIG. 2. Derivative of transmitted current vs electron energy in H_2. Four progressions of negative-ion states, are labeled as bands "*a*," "*c*," "*f*," and "*g*." The location of most likely parent electronic states of H_2 for bands "*a*" and "*c*" are indicated. Bands "*f*" and "*g*" are shown in the lower right-hand portion of the figure. For this portion of the scan, the gain has been increased by a factor of 7.

Band "*a*"

Sharp resonances in H_2 and its isotopes were first observed by Kuyatt, Simpson, and Mielczarek[11,12] who found two progressions of resonances in H_2 and HD and one progression in D_2, in the energy range 11–13 eV. The energetically lowest progression was designated "strong series" and corresponds to band "*a*" in our notation. Following this discovery, Heideman *et al.*[13] studied the energy dependence of the excitation cross sections to the first and second vibrational levels of the $B\,^1\Sigma_u^+$ state of H_2, and they related the sharp structures in their measurements to the resonances observed by Kuyatt *et al.* In the same energy range, Menendez and Holt[14] observed resonance structure in the forward electron scattering from H_2 into the $v=1$ and $v=2$ vibrational levels of the H_2 ground state. These authors were unable to state conclusively on the basis of their work, whether the two H_2^- bands found by Kuyatt *et al.* could fully account for the structure they observed.

Weingartshofer *et al.*,[15] in a detailed study of electron impact on H_2, investigated three progressions of resonances starting at 11.30, 11.50, and 13.63 eV. They designated the first two bands "series I" and "series II." "Series I" coincides in energy with band "*a*" and decays into all energetically possible exit channels.

Theoretical calculations initiated by Taylor and Williams[16] and improved by Eliezer *et al.*[17] predicted a total of four bands in the 11–13-eV energy range, one of which is band "*a*" with $^2\Sigma_g^+$ symmetry.

Comer and Read[18] investigated the 11–13-eV region by studying resonance progressions in the highly excited vibrational levels of the ground state of H_2 and D_2. By analyzing the measured cross sections, they were able to estimate three potential-energy curves of the H_2^- and D_2^- systems. They designated the bands they observed series "*a*," "*b*," and "*c*." In Table I we have adopted the same nomenclature. "Series *a*" or band "*a*" was assigned the $^2\Sigma_g^+$ symmetry from their analysis of angular distribution measurements, in agreement with the suggested symmetry deduced by Weingartshofer *et al.*[15]

Tables II and III list the energies of each vibrational level of band "*a*" as observed by various groups in H_2 and D_2, respectively. In Table II, the last column shows the theoretical values of Eliezer *et al.*[17] to which has been added 0.25 eV for the purpose of comparison. The possibility that experiments miss the $v=0$ level of band "*a*" must be dismissed since the starting energies for band "*a*" in H_2 and D_2 are identical. This would not be the case if the $v=0$ level would have been unobserved.

Our results for band "*a*" are listed in the first column of Tables II and III. The listed values are the energies of the progression of dips in the derivative of the transmitted current which appear between 11 and 13 eV in Fig. 2 and in Fig. 3, respectively. The dips are believed to lie energetically close to the resonance centers because they locate the largest slope in the resonance profile. A striking agreement exists between our results and the shifted theoretical values. The over-all agreement between various workers for band "*a*" in both H_2 and D_2 is very good, and the $^2\Sigma_g^+$ configuration for these H_2^- and D_2^- states seems well established.

It should be noted that resonance structure in molecular radiation from the $B\,^1\Sigma_u^+$ state of H_2 and D_2 upon impact with monoenergetic electrons has been observed[19,20] in the 11–13-eV region. Also in this region, structure has been observed[21] in the dissociative attachment channel which shows that a resonance progression can interact with a repulsive negative-ion state[17] and cause structure in the cross section for negative-ion formation by electron impact.

Band "*b*"

Band "*b*" has been observed only by Comer and Read[18] in high vibrational levels of the ground state

TABLE II. Comparison of the values obtained by different authors for the H_2^- states (eV).

Vibrational quantum number (H_2^-)	Transmission		Inelastic		Theory
	This work [a]	Kuyatt *et al.* [b]	Comer and Read *et al.* [c]	Weingartshofer *et al.* [d]	Eliezer *et al.* [e]
			Band "*a*" and "*d*"		
0	11.32	11.28	11.30	11.30	11.32
1	11.62	11.56	11.62	11.62	11.62
2	11.91	11.84	11.91	11.92	11.91
3	12.19	12.11	12.19	12.20	12.18
4	12.44	12.37	12.45	12.46	12.44
5	12.68	12.62	12.68	12.70	12.68
6		12.86	12.89	12.93	
7			13.10		
8			13.28		
			Band "*b*"		
1			11.27		
2			11.47		
3			11.63		
4			11.75		
5			11.85		
6			11.96		
			Band "*c*" and "*e*"		
0	11.43	11.46	11.37	11.50	11.46
1	11.74	11.72	11.71	11.79	11.75
2	12.03	11.99	11.99	12.08	12.03
3	12.32	12.27	12.21	12.38	12.31
4	12.58	12.53			12.58
5	12.83	12.77			12.84
6	13.06	12.97			
			Band "*f*"		
		Golden [f]			
0	13.66	13.62		13.63	
1	13.94	13.91		13.93	
2	14.20	14.19		14.20	
3	14.45	14.46		14.47	
4	14.69	14.72		14.70	
5	14.93	14.97		14.92	
6	15.18	15.21			
7	15.43	15.44			
8	15.65	15.66			
9	15.85	15.87			
10		16.07			
11		16.26			
			Band "*g*"		
	15.09				
	15.32				
	15.57				
	15.77				

[a] For bands "a" and "*f*" the minima in the derivative are given. For bands "*c*" and "*g*" the maxima are given.

[b] Data taken from Ref. 12.

[c] Data taken from Ref. 18 and private communication. The values for band "*c*" were derived by Comer and Read using their experimental values for the same band in D_2.

[d] Data taken from Ref. 15.

[e] We added 0.25 eV to the calculated values for band "*a*" for the purpose of comparison. The data were taken from Ref. 17.

[f] Data taken from Ref. 24.

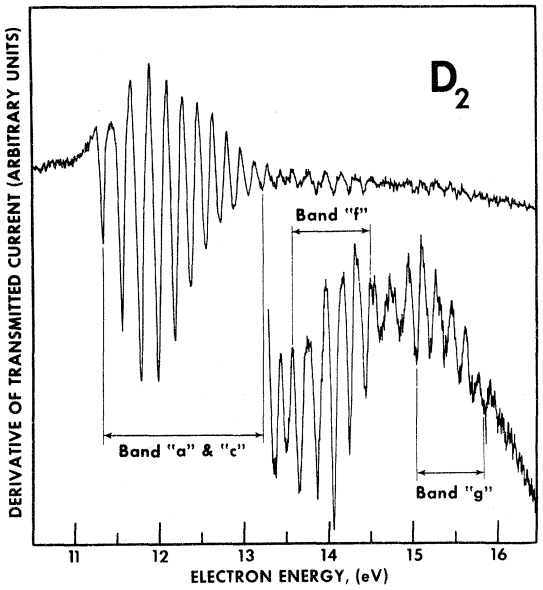

FIG. 3. Derivative of transmitted current vs electron energy in D_2. The bands have been designated on the figure. The gain has been increased by a factor of 10 for the trace shown on the lower right-hand portion of the figure.

TABLE III. Comparison of the values obtained by different authors for D_2^- states (eV).

Vibrational quantum number (D_2^-)	Transmission This work[a]	Transmission Kuyatt *et al.*[b]	Inelastic Comer and Read[c]
	Band "*a*"		
0	11.34	11.28	11.32
1	11.56	11.48	11.54
2	11.76	11.69	11.75
3	11.97	11.89	11.96
4	12.17	12.09	12.15
5	12.36	12.28	12.32
6	12.55	12.47	12.48
7	12.71	12.64	12.61
8	12.88	12.85	12.75
9	13.05		
10	13.22		
	Band "*c*"		
0	11.67		11.65
1	11.89		11.87
2	12.09		12.07
3	12.26		12.23
	This work only		
	Band "*f*"	Band "*g*"	
0	13.66	15.05	
1	13.86	15.22	
2	14.06	15.39	
3	14.25	15.55	
4	14.43	15.71	
5	14.57		

[a]For bands "*a*" and "*f*" minima in the derivatives are given. For bands "*c*" and "*g*" maxima are given.

[b]Data taken from Ref. 12.

[c]Data taken from Ref. 18.

of H_2. They obtained a natural width of 30 meV for band "*b*" and suggested that the new resonance has the configuration $(\sigma_g 1s)(\sigma_u 1s)^2\,{}^2\Sigma_g^+$, representing an electron bound to the $B\,{}^1\Sigma_u^+$ excited state of H_2. This band has not been observed in any transmission experiment.

Band "*c*"

Band "*c*" has been observed in the transmission experiments of Kuyatt *et al.*,[12] and it is also observed in the present experiment as a progression of peaks between 11 and 13 eV. Band "*c*" also appears in D_2 on high-resolution runs. Such a run is shown in Fig. 4 on an extended energy scale, where it is shown that band "*a*" is perturbed by the presence of four peaks (indicated by vertical arrows) which belong to band "*c*."

Eliezer *et al.*[17] calculate a $^2\Sigma_g^+$ state lying above "*a*" and starting at 11.46 eV. Their computed values for the vibrational levels of this $^2\Sigma_g^+$ state appear on the last column in Table II under the heading of band "*c*" and "*e*". The agreement between the theoretical values and ours is seen to be very good. Thus band "*c*" observed in the present work is probably due to the 11.46-eV $^2\Sigma_g^+$ state.[17] This interpretation has been advanced by Kuyatt *et al.*[12]

Comer and Read[18] observed (in D_2 only) a band coincident in energy with band "*c*." They determined the potential-energy curve for the state re-

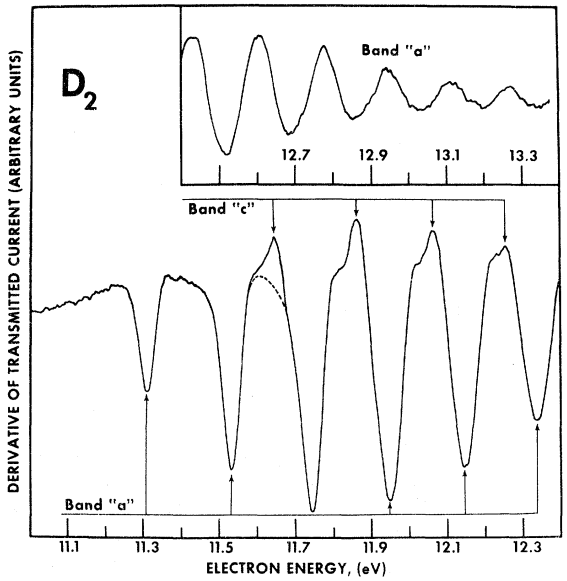

FIG. 4. Derivative of transmitted current vs electron energy in the region 11–13 eV in D_2 plotted on an extended energy scale. The dashed line, traced between the second and third dips of band "*a*," represents the expected shape of the spectrum if band "*c*" were not present. The upper right-hand insert is a continuation of band "*a*."

sponsible for this band and assigned to it the configuration $(\sigma_g 1s)(\pi_u 2p)(\sigma_g 2s)\ ^2\Pi_u$. Surprisingly, they did not observe this progression in H_2, although the predicted cross section for H_2, derived from their deuterium data was relatively large. They calculated the expected energy values for band "*c*" in H_2, and Table II shows that the calculated values are within 100 meV of our measured values. Nevertheless, it is probable that the $^2\Pi_u$ band of Comer and Read is not band "*c*" observed in the present work.

Tables II and III show a comparison of our energy values with the results of other investigators. The agreement is seen to be good.

Band "*d*"

This band was postulated by Comer and Read[18] from an analysis of the results of Weingartshofer *et al.*[15] On the basis of the angular distribution of electrons observed by Weingartshofer *et al.* in the $B\,^1\Sigma_u^+$ exit channel, Comer and Read suggest that the compound state involved must have $^2\Pi_g$ symmetry. Although the results of Weingartshofer are coincident in energy with series "*a*," Comer and Read suggest that the compound state is not the same, since series "*a*" involves a $^2\Sigma_g^+$ state. However, Black and Lane[22] have recently pointed out that angular distributions are not a simple guide to the assignment of symmetries, because different rotational transitions may be dominant in various decay channels. Thus Black and Lane show that the rotational transition $j=0\rightarrow j=1$ dominates in the process

$$e+H_2(X\,^1\Sigma_g^+)\rightarrow H_2^-(e+C\,^1\Pi_u)\rightarrow H_2(B\,^1\Sigma_u^+)+e\ .$$

If such mechanisms are present, angular distributions will have to be analyzed in more detail. The possible equivalence of band "*a*" and "*d*" is shown by arrows on the top of Table I.

Band "*e*"

Under the heading of band "*e*" we list the measurement of Weingartshofer *et al.*[15] who observed inelastically scattered electrons having excited the $B\,^1\Sigma_u^+$ state. As in the case of series "*c*," Comer and Read[18] assert that the anisotropic nature of the angular distribution observed by Weingartshofer *et al.* is not compatible with the assignment of series "*c*." But series "*e*" is nearly coincident in energy with series "*c*." As discussed in the preceding paragraph, it is possible that a proper interpretation will come to the conclusion that series "*c*" and "*e*" are identical.

Bands "*f*" and "*g*"

Band "*f*" extends from approximately 13.5 to 16 eV in H_2 and from 13.5 to 14.5 eV in D_2 and appears in Figs. 2 and 3, respectively. In each figure, a higher sensitivity run showing band "*f*" is traced in the lower right-hand portion. This band corresponds to the 13.63-eV progression found by Ehrhardt and Weingartshofer[23] in H_2, which has been recently observed by Golden[24] in a transmission experiment using a derivative technique similar to ours. The results obtained by these authors are compared with those of the present experiment in Table II. The minimum points in our derivative curve are also given in Table II. Band "*f*" exhibits a width of about 90 meV in both H_2 and D_2, in good agreement with the natural width of 80 meV estimated by Ehrhardt *et al.*[23] The $^2\Sigma_g^+$ symmetry for band "*f*" was assigned by these authors.

Figure 2 shows that band "*f*" appears perturbed by the presence of other structures. We do not feel that this perturbation could be explained in terms of interference effects between resonant and nonresonant scattering, since the potential scattering, which influences the shape of the resonance, is not expected to change considerably over the energy range of the progression. In H_2, at least four members of a perturbing progression can be observed in our experiment. This new band is labeled "*g*" and tabulated in Table II. It appears much more clearly in D_2 (Fig. 3) where bands "*f*" and "*g*" do not overlap. The energy of each member of band "*g*" for D_2 is listed in Table III. Three features around 16 eV in the data of Golden[24] in H_2, which he attributed to autoionization, could be members of band "*g*."

Definite band assignment in H_2 and its isotopes will require further theoretical and experimental investigations. In particular, special attention must be given to the role played by rotational transitions in the interpretation of angular distribution experiments.

V. RESULTS IN O_2

The electron transmission spectrum of O_2 in the 8–13-eV region is shown in Fig. 5 on which each structure is labeled. Table IV lists the energies of these structures.

Structures (1-1′) to (17-17′)

Structures (1-1′) and (3-3′) have been identified as resonances in our previous work.[25] The two resonances appear to be extremely narrow. Experiments with increased resolution show the measured width at half-maximum of the two resonances to be 20 meV and still limited by instrumental resolution and Doppler broadening. From these measurements we estimate the natural width of the two resonances to be less than 10 meV.

The spacing between resonance (1-1′) and (3-3′) is 220 ± 5 meV, and this value compares with the spacing[26] for the first two vibrational levels of the

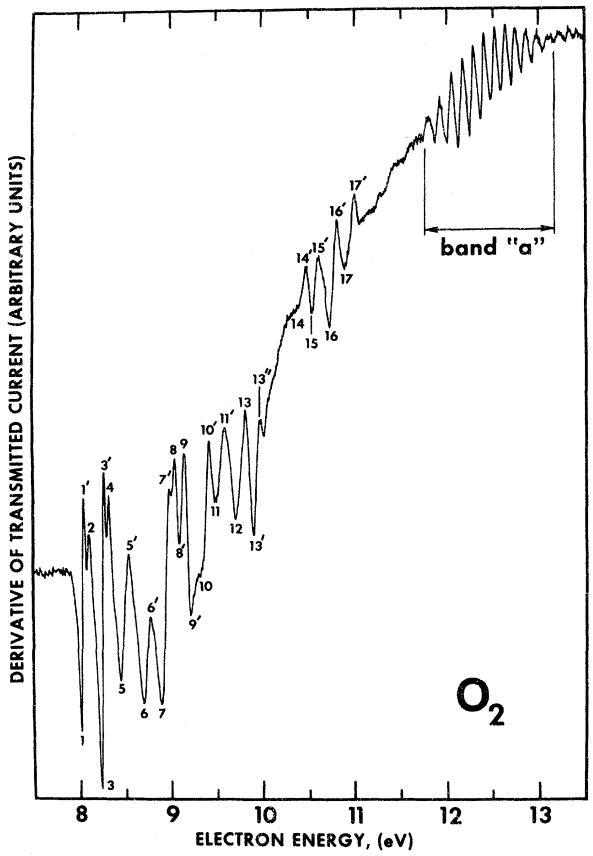

FIG. 5. Derivative of transmitted current vs electron energy in O_2. Structures 1 to 17 are interpreted as resonances whose grandparent is the ground state of O_2^+. A well-developed progression of ten resonances called band "a" appears near the end of the spectrum. The $a\,^4\Pi_u$ state of O_2^+ is the grandparent of band "a."

$X^2\Pi_g$ core of O_2^+ which is 232 meV. We therefore suggest that the resonances (1-1′) and (3-3′) consist of two Rydberg electrons bound to the $X^2\Pi_g$ ionic core. Furthermore the ratio of the magnitudes of resonance (3-3′) and (1-1′) gives a value of 1.36, which compares with the value of 1.97 for the corresponding ratio of the Franck-Condon probabilities[27,28] for excitation of the first two vibrational states of the $X^2\Pi_g$ core of O_2^+.

The likely parents of the core-excited resonance could be formed by the addition of an electron having the $3s\sigma_g$ Rydberg orbital symmetry to the $X^2\Pi_g$ positive-ion core, thus forming $^3\Pi$ and $^1\Pi$ Rydberg states. The addition of another $3s\sigma_g$ electron to the $^3\Pi$ or the $^1\Pi$ state of O_2 can give a $^2\Pi_g$ symmetry, which is the suggested designation for the two observed vibrational members of the O_2^- progression.

The Franck-Condon probabilities[27] for excitation of the $v=2$, 3, and 4 levels of the $X\,^2\Pi_g$ core of O_2^+ are relatively large and therefore, it is surprising that we do not observe vibrational members higher than the first for the O_2^- progression. Accurate measurements of the spacings between structures 5-5′, 6-6′, and 7-7′ indicate that these resonances do not form a regular progression with structures 1-1′, 2, 3-3′, and 4. It is possible that the O_2^- vibrational progression is predissociated above the first vibrational level. A hypothetical situation, leading to predissociation, is shown by the potential-energy curve diagram of Fig. 6. The potential-energy curve $R(XY^-)$ to which resonances (1-1′) and (3-3′) are assumed to belong is crossed near 8.3 eV by a valence negative-ion potential-energy curve $V(XY^-)$ of the same symmetry. The avoided crossing between these states creates a potential-energy curve with a potential "hump" which can support only two vibrational levels [i.e., resonances (1-1′) and (3-3′)]. Curve $R(XY)$ represents the parent of the curve $R(XY^-)$, and it can be represented by a potential-energy curve having about the same shape as curve $R(XY^-)$ and lying approximately 0.5 eV above it. The repulsive negative-ion curve $V(XY^-)$ also has a parent which is represented in the figure by the dashed curve $V(XY)$. Although state $R(XY)$ is completely predissociated by an avoided crossing with curve $V(XY)$, the interaction between the negative-ion potential-energy curve $R(XY^-)$ and $V(XY^-)$ occurs at a different energy and permits observation of two vibrational levels of the O_2^- compound state. This reasoning shows that a parent state (e.g., the lowest $^3\Pi$ Rydberg state of O_2) could be broadened,

TABLE IV. Features in O_2 (8–11 eV).

1–1′	2	3-3′	4	5–5′
8.03–8.06	8.12	8.24–8.28	8.34	8.47–8.54
6–6′	7–7′	8–8′	9–9′	10–10′
8.71–8.78	8.90–8.98	9.08–9.11	9.16–9.23	9.36–9.44
11–11′	12	13–13′–13″	14–14′	15–15′
9.53–9.61	9.73	9.86–9.92–9.98	10.43–10.48	10.55–10.61
16–16′	17–17′			
10.74–10.82	10.91–11.00			

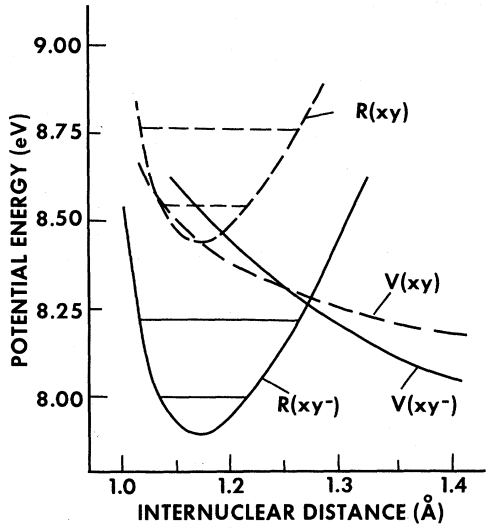

FIG. 6. Hypothetical potential-energy diagram drawn to explain the sudden cutoff of bands. The two solid curves indicate hypothetical energy curves of the same symmetry of an XY^- system, and the dashed curves are curves for the neutral molecule. The Rydberg state $R(XY)$ is the parent of the compound state $R(XY^-)$, and the valence state $V(XY)$ is the parent of the compound state $V(XY^-)$. The crossings lead to predissociation of the states $R(XY^-)$ and $R(XY)$.

whereas some levels of the compound state (e.g., the $^2\Pi_g$ state of O_2^-) could remain sharp.

Structures 2 and 4 lie 40 ± 5 meV above structures 1-1′ and 3-3′, respectively. They could reflect spin-orbit splitting of the $^2\Pi_g$ state of O_2^- into a $^2\Pi_{3/2}$ configuration for resonances (1-1′) and (3-3′) and a $^2\Pi_{1/2}$ configuration for resonances 2 and 4. The observed doublet spacing appears larger than the value of 24 meV for the splitting[26] of the ground state of O_2^+, possibly because of the overlap of the two resonances.

The next portion of the transmission spectrum shows many structures labeled from 5 to 13 which do not form a regular progression. The structures seem to possess an appreciable amount of overlap and apparent widths of about 80 meV. They could result from the many other Rydberg negative ions which can be formed in this energy region by the attachment of two Rydberg electrons to the grandparent $X^2\Pi_g$ core of O_2^+. If many overlapping resonances are thus formed, the observed widths may bear little relation to the natural width of each resonance,[29] and the resulting structures may not exhibit the usual regularity inherent in band progressions.

The next group of resonances (14 to 17′) could possibly form a progression, but it is more difficult in this case to identify them. The complexity of the O_2^- resonance structure in this energy range parallel the complexity of the O_2 absorption spectrum in the same energy region.

Band "a"

At higher energies, a well-developed progression of ten resonances appears in the spectrum starting at 11.81 ± 0.05 eV. We have recently reported[30] a study of this progression which we call band *"a."* Table V shows a comparison between vibrational spacings and Franck-Condon probabilities of band *"a"* and those[26,28] of the $a^4\Pi_u$ grandparent state of O_2^+. No such correspondence can be found if the experimental data are compared with other states of O_2^+, i.e., the $X^2\Pi_g$, $A^2\Pi_u$, $b^4\Sigma_g^-$, and $B^2\Sigma_g^-$ states of O_2^+.

TABLE V. Comparison of vibrational spacings and Franck-Condon probabilities observed for band *"a"* in O_2^- found in the present experiment with the appropriate values for O_2^+ ($a^4\Pi_u$). The symbol × means "not observed".

	Vibrational spacings (meV)		Franck-Condon probabilities	
v	O_2^+ ($a^4\Pi_u$) $(v-1)\rightarrow v$ [a]	O_2^- $(v-1)\rightarrow v$ [b]	$O_2(X^3\Sigma_g^-,\ v'=0)\rightarrow O_2^+$ ($a^4\Pi_u$, v) [c]	$O_2(X^3\Sigma_g^-,\ v=0)\rightarrow O_2^-$ (v) [d]
0	...	...	0.076	×
1	126	×	0.278	0.298
2	123	124	0.561	0.447
3	121	122	0.819	0.765
4	118	120	0.986	1.000
5	115	116	1.000	0.980
6	113	113	0.921	0.893
7	110	110	0.783	0.724
8	108	110	0.621	0.596
9	105	107	0.470	0.510
10	103	109	0.341	0.340

[a]Values for the vibrational spacings for the O_2^+ ($a^4\Pi_u$) state from Ref. 26.

[b]The estimated error for the experimental vibrational spacings for O_2^- is ± 0.003 eV.

[c]Values for the Franck-Condon probabilities for the O_2^+ ($a^4\Pi_u$) state from Ref. 28.

[d]The estimated error for the experimental Franck-Condon probabilities for O_2^- is ± 20%.

The quantum number of each vibrational level of the O_2^- state is determined by fitting the Franck-Condon probabilities of the O_2^- ion to those of the O_2^+ ion. The zeroth level of the O_2^- progression cannot be observed because its Franck-Condon probability is small. The comparison of Table V clearly indicate that the O_2^+ and O_2^- ions have essentially identical potential-energy curves. This suggests that band "a" results from vibrational structure of a $^4\Pi_u$ Rydberg negative ion, formed by the addition of two Rydberg electrons of the $3s\sigma_g$ orbital symmetry to a O_2^+ core in the $a\,^4\Pi_u$ valence excited state. The likely parents of the O_2^- state could be formed by the addition of a single $3s\sigma_g$ electron to the $O_2^+(a\,^4\Pi_u)$ core, thus forming $^3\Pi$ and $^5\Pi$ Rydberg states. These states lie[31] at 12.50 eV ($^3\Pi$) and 12.24 eV ($^5\Pi$), respectively, and the observed progression lies about 0.6 eV below the $^5\Pi$ state. Since a value of 0.6 eV is a reasonable value for the electron affinity, we consider this a further confirmation that the $^{3,5}\Pi$ states of O_2 are the parents of band "a."

Band "b" (not shown in Fig. 5)

Another band of O_2^- states (band "b"), consisting of a progression of four vibrational members, has been observed above ionization. The levels lie at 14.27, 14.43, 14.58, and 14.72 ± 0.1 eV, respectively. In this case the vibrational spacings are close to those[26] of the $b\,^4\Sigma_g^-$ state of O_2^+. The $^3\Sigma_u^-$ state which lies 0.210 eV above the zeroth level of band "b" and constitutes the lowest Rydberg excited state belonging to the $b\,^4\Sigma_g^-$ state of the positive-ion system is the suggested parent for this progression.

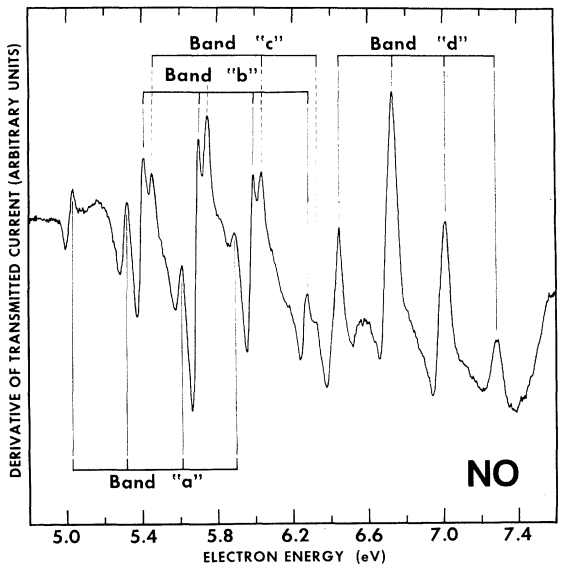

FIG. 7. Derivative of transmitted current vs electron energy in the 5–7.5-eV region in NO. Four bands belonging to a Rydberg series of NO^- states are shown; each band consists of a vibrational progression. The spacing of each vibrational progression agrees with the vibrational spacing of the $X\,^1\Sigma^+$ ground state of NO^+, which is the grandparent.

TABLE VI. Comparison of vibrational spacings and Franck-Condon probabilities observed for four bands of NO^- in the present experiment with appropriate values for NO^+ ($X\,^1\Sigma^+$).

	Vibrational spacings (meV)					
	NO^- band				NO^+ ($X'\,\Sigma^+$)	
Δv	"a"	"b"	"c"	"d"	Expt[a]	
0–1	286	290	292	282	290	
1–2	286	290	288	284	287	
2–3	282	284	286	275	283	
3–4				275	278	
4–5				275	273	
	Franck-Condon probabilities					
	NO^- band				NO^+ ($X'\,\Sigma^+$)	
v	"a"	"b"	"c"	"d"	Expt[b]	Theoret[c]
0	0.84	0.57	···	0.66	0.7	0.48
1	1	1	···	1	1	1
2	0.62	0.64	···	0.7	0.7	0.92
3	0.16	0.24	···	0.19	0.5	0.49

[a]Experimental values for the NO^+ ($X\,^1\Sigma^+$) state from Ref. 32.

[b]Experimental values for the Franck-Condon probability of NO^+ ($X\,^1\Sigma^+$) from H. Hurzeler, M. G. Inghram, and J. D. Morrison, J. Chem. Phys. 28, 76 (1958).

[c]Theoretical values for the Franck-Condon probability for NO^+ ($X\,^1\Sigma^+$) from Ref. 28. "a," "b," "c," and "d" represent designations of bands (see Fig. 7), which start at 5.04, 5.41, 5.46, and 6.44 ± 0.05 eV, respectively.

VI. RESULTS IN NO

Figure 7 shows a plot of the derivative of the transmitted current versus electron energy for NO in the 5–7.5-eV energy range.

Bands "a" to "d"

The location of four bands[30] of resonances "a"–"d" is indicated by vertical lines pointing to each vibrational member for a given band. Each of the first three bands has four vibrational members, and the bands start at 5.04, 5.41, and 5.46 eV, respectively. Band "d" starts at 6.45 eV, and six vibronic states belonging to that band have been observed; four of these are shown in Fig. 7. The vibrational spacings of each band and the Franck-Condon probabilities for band "a", "b", and "d" are compared with the corresponding values[26,28,32] for the $X\,^1\Sigma^+$ ground state of NO^+ in Table VI. Bands "a"–"c" have about the same spacing, which agrees well with the spacing[26,32] of the grandparent NO^+ core. Band "d" deviates slightly from the

grandparent spacing. Franck-Condon probabilities for bands "*a*," "*b*," and "*d*" agree qualitatively with those of the NO^+ ion core,[28] even though bands "*a*," "*b*," and "*c*" overlap. All Franck-Condon probabilities listed are normalized to $v=1$ for comparison purposes.

The comparisons of Table VI suggest that all four bands in NO are composed of two Rydberg electrons temporarily bound to the same $X\,^1\Sigma^+$ core of NO^+. The parent of band "*a*" is probably the $A\,^2\Sigma^+$ Rydberg state[33] of NO which lies at 5.48 eV.[26] The *A* state, whose electron affinity from the above argument is 0.45 eV, corresponds to an electron in a Rydberg orbital of the symmetry $3s\sigma$ bound to the $X\,^1\Sigma^+$ core of NO^+. The addition of another $3s\sigma$ electron to the core gives the $^1\Sigma^+$ symmetry for band "*a*."

Bands "*b*" and "*c*," which lie 0.07 and 0.02 eV below the $A\,^2\Sigma^+$ state of NO, respectively, could result from the addition of a $3p\sigma$ or $3p\pi$ electron to the *A* state. In this case, the potential well which forms band "*a*" would posses two other energy levels at 5.41 and 5.46 eV and give rise to bands "*b*" and "*c*." Alternatively, the parents of bands "*b*" and "*c*" could be the $C\,^2\Pi$ and $D\,^2\Sigma^+$ states of NO, which lie[26] at 6.49 and 6.60 eV, respectively. As far as band "*d*" is concerned, the likely parents are only the *C* and *D* states of NO. The *C* state is composed of a $X\,^1\Sigma^+$ core of NO^+ which binds a $3p\sigma$ electron. In the *D* state, the Rydberg electron has the $3p\pi$ orbital configuration. Addition of another electron in any of the $n=3$ Rydberg energy levels to the *C* or *D* states leads to a large number of possible states of NO^-, and it is difficult, without calculations, to determine which of these states are bound. The fact that singlet and triplet compound states can be formed adds to the complexity.

Paquet, Marchand, and Marmet[34] have recently postulated the presence of two long-lived bound negative-ion states at 7.8 and 8.2 eV, in order to explain two peaks they observe in the cross section for O^- formation from NO at these energies. The postulated states should appear in the total scattering cross section. We did not observe any structure at 8.2 eV, but the fifth vibrational member of band "*d*" which lies at 7.83 eV could possibly account for the 7.8-eV peak in the O^- data of Paquet *et al.*

Region 12-20 eV

In the 12–20-eV energy range, we expect to observe other sharp resonances in the total scattering cross section of NO which have as their grandparents *excited* states of NO^+. At least ten bound excited states of NO^+ are known at the present time,[35] and four of these, namely, the $b\,^3\Pi$, $A\,^1\Pi$, $c\,^3\Pi$, and $B\,^1\Pi$ ion states, can be considered as possible candidates for compound-state formation from the ground state since their internuclear distances lie close to the internuclear distance of the NO ground state. The *b*, *A*, *c*, and *B* ion states lie[35] at 16.56, 18.32, 20.46, and 21.72 eV above the ground state of NO. We can predict approximately the energy of the energetically lowest resonance associated with each of these excited states of NO^+ by simply adding to the energy of band "*a*" the electronic excitation energy of the *b*, *A*, *c*, and *B* states of NO^+. This procedure assumes that the potential well which binds the two $3s\sigma$ electrons to the $X\,^1\Sigma^+$ core of NO^+ for band "*a*" remains unaltered when the valence configuration or symmetry of the ion core is changed. Also, this procedure predicts only the energy of the zeroth vibrational level of the negative-ion states which consist of two $3s\sigma$ electrons of opposite spin trapped in the field of the respective *b*, *A*, *c*, and *B* grandparent cores. Such an estimate gives 12.33, 14.10, 16.23, and 17.55 eV for the compound states associated with the *b*, *A*, *c*, and *B* grandparents, respectively. Experimentally (see Fig. 8), we observe structure at 12.36, 14.19, and 17.51 ± 0.05 eV, in excellent agreement with the predicted energy values.

No resonances corresponding to the $c\,^3\Pi$ grandparent are observed. This finding corroborates the results of Edqvist *et al.*[35] who measured the intensity of the photoelectron peak produced upon excitation of the $c\,^3\Pi$ state to be only 0.1% of the $B\,^1\Pi$ peak.[36] Samson,[37] who has also studied the photoelectron spectrum of NO by use of retarding poten-

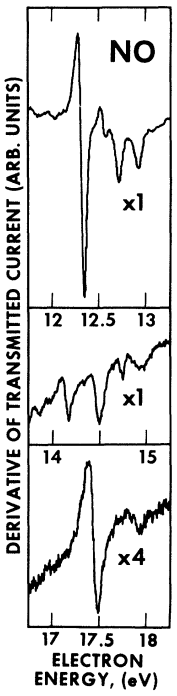

FIG. 8. Electron transmission spectra for NO in the 12–13-, 14–15-, and 17–18-eV regions. Each spectrum shows resonances associated with the $b\,^3\Pi$, $A\,^1\Pi$, and $B\,^1\Pi$ excited states of NO^+, which are the respective grandparents. The binding of the first compound state in each spectrum relative to the corresponding grandparent state is nearly constant.

tials, could not detect the $c\,^3\Pi$ state. As expected, the strongest peaks in the photoelectron spectrum of NO are associated with excitation of NO^+ states (i. e., the b, A, and B states) which are the grandparents of the largest resonances in our electron transmission spectra.

The 12.36-eV resonance appears as the first structure on the upper portion of Fig. 8 where it exhibits a rise followed by a sharp decrease in the derivative of the transmitted current. The $v=1$ level of that resonance lies at 12.57 eV on our curve. Its intensity is nine times smaller than the intensity of the zeroth level at 12.36 eV, in good agreement with the value of ten for the corresponding ratio of intensities for exciting the $v=0$ and 1 vibronic levels[35] of the $b\,^3\Pi$ core of NO^+. The parent Rydberg states probably have the $^4\Pi$ and $^2\Pi$ symmetries. The quartet state would lie at approximately 12.8 eV.

The last two structures[38] shown in the upper portion of Fig. 8 have their minimum in the derivative curve at 12.73 and 12.94 eV. They could arise from a p-wave core-excited shape resonance of the type encountered in rare-gas atoms.[3,8,39] If such a negative-ion complex is formed in a diatomic molecule, the captured p-wave electron is expected to adopt either the σ or the π orbital symmetry depending on its angular momentum about the internuclear axis. Thus two resonances should actually be observed. This type of resonant process is further discussed in the text in connection with the N_2 transmission spectra.

Two resonances associated with the $A\,^1\Pi$ valence excited state of NO^+ can be seen in the middle portion of Fig. 8. These structures have their minimum in the derivative transmission curve at 14.19 and 14.52 eV, respectively. The parent NO state of the two resonances would be a $^2\Pi$ Rydberg state corresponding to an electron in a Rydberg orbital of the symmetry $3s\sigma$ bound to the $A\,^1\Pi$ core of NO^+. The addition of another $3s\sigma$ electron to the A core would give a $^1\Pi$ symmetry for the 14.19-eV resonance. The other resonance at 14.52 eV probably results from a $(3s\sigma)\,(3p\sigma)$ or a $(3s\sigma)\,(3p\pi)$ configuration of the Rydberg electrons.

The energetically lowest compound state having the $B\,^1\Pi$ state of NO^+ as the grandparent is shown in the lower portion of Fig. 8. This negative-ion state has a natural width of about 110 meV as evidenced by the positions of the maximum and minimum at 17.40 and 17.51 eV, respectively, in the derivative curve. The dip which appears at 17.94 eV could result from another doubly excited Rydberg negative ion belonging to the same grandparent or, less likely, from a sharp inelastic onset. No other sharp structures beyond those shown in Fig. 8 have been observed between 12 and 20 eV with the present sensitivity.

An energy-level diagram of the zeroth vibronic level of each NO^- state observed in this work is shown on the right-hand side of Fig. 9. On the left-hand side of this figure we show the energy levels of the NO^+ grandparent states. The two scales have been displaced by the difference in energies between the lowest member of band "a" with respect to its grandparent, the $X\,^1\Sigma^+$ core of NO^+ (4.23 eV), in order to show the relationship between the NO^+ states and its grandchildren NO^- states. This comparison demonstrates that the binding energy of two $3s\sigma$ Rydberg electrons does not depend on the configuration of the positive-ion core. It also illustrates that in NO only Rydberg excited states give rise to core-excited resonances in the total scattering cross section.

VII. RESULTS IN N_2

Figure 10 shows a plot of the derivative of the transmitted current versus the electron energy in N_2 in the energy range 11–15 eV. The energy of the most pronounced structures are listed in Table VII which also shows a comparison with the values obtained by Comer and Read[40] (differential elastic and inelastic cross section), Hall *et al.*[41] (trapped

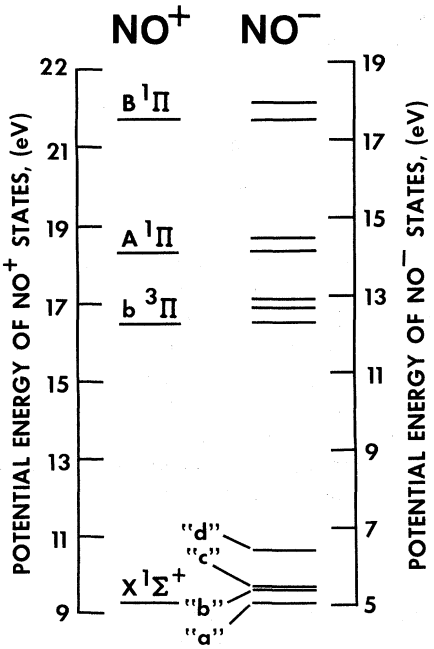

FIG. 9. Energy-level diagram of relevant NO^+ grandparent states (left-hand side of diagram) compared with the energy-level diagram of the NO^- state observed in the present experiment (right-hand side of diagram). The two energy scales have been displaced by the binding energy of the lowest member of band "a" with respect to its grandparent $X\,^1\Sigma^+$ state of NO^+. Each state of NO^+, shown on the left-hand side of the diagram, gives rise to a Rydberg series of NO^- states.

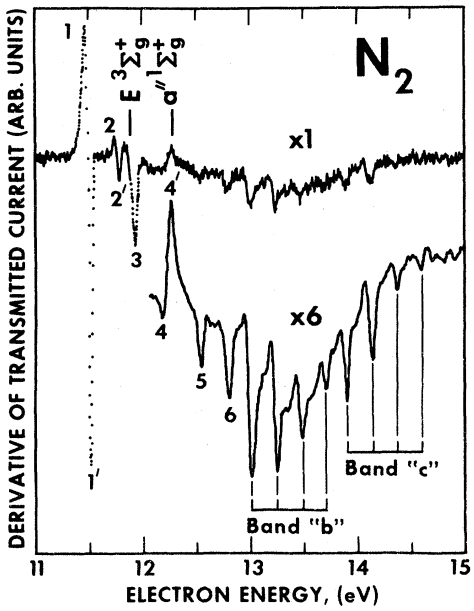

FIG. 10. Derivative of transmitted current vs electron energy in N_2. The giant resonance $1-1'$ is a $^2\Sigma_g^+$, N_2^- state whose parents are the $E\,^3\Sigma_g^+$ and $a''\,\Sigma_g^+$ Rydberg states of N_2. The grandparent of structures 1–4 is the ground state of N_2^+. The other resonances, including bands "c" and "d" which appear on the higher-sensitivity run at the bottom of the figure, have the $A\,^2\Pi_u$ state of N_2^+ as grandparent.

electrons), and Heideman *et al.*[42] (transmission).

Structures (1-1′) to (4-4′)

Structures (1-1′) to 3 in N_2 were first observed in a conventional transmission experiment by Heideman *et al.*[42] These authors suggested that structures (1-1′) and (2-2′) were the zeroth and first vibrational members of a temporary negative-ion state. Our values for the zero level in the derivative curve are 11.49 ± 0.03 and 11.76 ± 0.03 eV, respectively, in excellent agreement with the values of 11.48 and 11.75 eV found by Heideman *et al.* for these two states. Comer and Read[40] observe a third member of the above progression at 12.02 eV in a scattering experiment in which the exit channel is a vibrational level of the ground state. We refer to this progression as band "*b*."

Comer and Read[40] deduce from the analysis of band "*b*" the potential-energy curve of the N_2^- state involved, and they estimate the natural width of the resonance to be only 0.6 meV. Their angular distribution studies indicate that the scattering is predominantly *s* wave in nature. This result suggests a $^2\Sigma_g^+$ symmetry for the compound state. The most likely parents are the $E^3\Sigma_g^+$ and $a''\,^1\Sigma_g^+$ states of N_2 whose potential-energy curves resemble closely the one obtained by these authors for the $^2\Sigma_g^+$ negative-ion state. Comer and Read point out that the fact that the *E* state is a Rydberg state supports the Weiss-Krauss theory[9] on the Rydberg nature of core-excited resonances in molecules. In fact, the $^2\Sigma_g^+$ resonance consists of two electrons of the Rydberg orbital symmetry $3s\sigma_g$ temporarily bound in the field of the grandparent $X\,^2\Sigma_g^+$ core of N_2^+. This is evidenced in the present experiment by the fact that both the spacing between the zeroth and first vibrational level of band "*b*" and the amplitudes of the structures are close in magnitude to the corresponding values[26,43] for excitation of the ground state $X\,^2\Sigma_g^+$ of N_2^+. In fact, we observe a spacing of 270 ± 3 meV between structures (1-1′) and (2-2′) and a ratio of magnitudes between the two of 10 ± 0.5. These findings agree extremely well with the values for the $X\,^2\Sigma_g^+$ state of N_2^+, which has a spacing of 271 meV between the $v=0$ and $v=1$ states and which has a ratio of 9.96 for the Franck-Condon probabilities for exciting these vibronic states.

Since only the zeroth level of the $X\,^2\Sigma_g^+$ grandparent state is strongly excited in molecular transitions from the ground state of N_2, we do not expect other smaller resonances which might be associated with the $X\,^2\Sigma_g^+$ grandparent to form visible progressions. The next two resonances, structures 3 and 4-4′, appear isolated and should be considered as grandchildren of the $X\,^2\Sigma_g^+$ state of N_2^+. We can thus speculate that structures 3 and 4-4′ are the *p*-wave resonances associated with the $E\,^3\Sigma_g^+$

TABLE VII. Features in N_2 (11–13 eV).

Feature number	Transmission (this work)	Transmission (Heideman *et al.*) (Ref. 42)	Differential elastic and inelastic (Comer and Read) (Ref. 40)	Trapped electron (Hall *et al.*) (Ref. 41)
1−1′	11.47–11.51	11.48	11.48	
2−2′	11.74–11.78	11.75	11.755	
			12.02	
3	11.92	11.87	11.87	11.87
4−4′	12.18–12.27		12.205	12.25
5	12.64			
6	12.87			

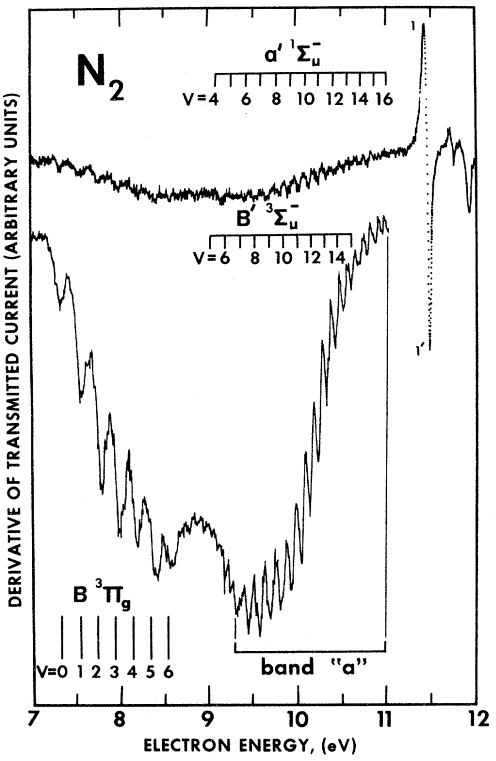

FIG. 11. Electron transmission spectra in the 7–11-eV energy range in N_2. Structure in the region 7–9 eV is due to inelastic processes involving the $B\,^3\Pi_g$ state of N_2. The location of the $B\,^3\Pi_g$ state, the $B'^3\Sigma_u^-$ state and the $a\,^1\Sigma_u^-$ state of N_2 are indicated. Band "*a*" does not seem to result from an inelastic process associated with any known electronic state of N_2. Therefore we postulate that band "*a*" results from a compound state whose parent is a valence state. The origin of this band is a mystery.

and $a''\,^1\Sigma_g^+$ parent Rydberg states of N_2. Many other Rydberg states[26,44] of N_2 also consist of a Rydberg electron bound by the field of the $X\,^2\Sigma_g^+$ core of N_2^+, but they cannot be considered as parents of resonances 3 and 4-4′ because their energies lead to unreasonable electron affinities.

The *p*-wave core-excited resonance of the type suggested to explain the presence of structures 3 and (4-4′) is well established[8,39] for the case of He, where a ^2P resonance exists just above the parent, $2\,^3S$ excited state. In Ne, Ar, Kr, and Xe, there also occurs structure above the first inelastic onset which could be interpreted as a *p*-wave core-excited shape resonance (core-excited type II) whose parent is the lowest excited state of the respective neutral rare-gas atom.[3] If the same phenomenon occurs in the N_2 Rydberg system, the *p*-wave resonance would split into two negative-ion states of the Σ and Π symmetry giving rise to resonances 3 and 4-4′, respectively. Elastic scattering from these two states disappears at an angle of 85° showing consistency with the *p*-wave interpretation advanced above.[40]

It is known from studies[8,39] of core-excited shape resonances in helium that these resonances decay strongly into their parents and enhance their excitation function. In the case of N_2, Swanson *et al.*[45] and Ehrhardt and Willmann[46] have detected enhancement of the excitation function of the $E\,^3\Sigma_g^+$ and the $a''\,\Sigma_g^+$ parents near the energy of the Σ and Π resonances. No resonance effects were observed in the excitation function of any other states in the 10–12-eV range.[45] Resonance 4-4′ also affects the total metastable production in N_2 as evidenced by a peak at about 12.2 eV in the data of Borst and Zipf,[47] of Clampitt and Newton[48] and of Olmsted *et al.*[49] Electron impact experiments using the trapped-electron method show similar results.[41,50]

Structures 5 and 6

The energy of the lowest compound state composed of two Rydberg electrons trapped in the field of the $A\,^2\Pi_u$ core of N_2^+ can be estimated by adding to the energy position of resonance (1-1′) the difference between the ionization potential for the $X\,^2\Sigma_g^+$ and the $A\,^2\Pi_u$ states of N_2^+. Such an estimate gives 12.62 eV for the energy position of that $^2\Pi_u$ resonant state which would consist of two $3s\sigma_g$ electrons bound to the $A\,^2\Pi_u$ core. Resonances 5 and 6 probably belong to that state. In fact, resonance 5 lies at 12.64 eV, only 20 meV above the estimated position.

Bands "*c*" and "*d*"

Two short bands ("*c*" and "*d*") appear in the 13–15-eV energy range in N_2. They start at 13.00 and 13.88 ± 0.05 eV, respectively. Here the overlap between the different resonances makes an accurate reading of the spacing between the vibrational members of each band difficult. Nevertheless, the average spacing of 230 ± 5 meV for band "*c*" and 225 ± 5 meV for band "*d*" lies close to the value of 228 meV for the corresponding *average* spacings of the vibrational levels[26] of the $A\,^2\Pi_u$ state of N_2^+ which is the suggested grandparent for the two bands.

Excitation of the $B\,^3\Pi$ state and band "*a*"

At lower energies (7–11 eV), other structures are visible in the total scattering cross section of N_2. These structures are clearly seen in derivative transmission spectra for N_2 shown in Fig. 11. The progression of dips between 7 and 9 eV is interpreted as the excitation of vibrational levels of the $B\,^3\Pi_g$ valence state of N_2 and indicates that the cross section for excitation of the *B* state rises sharply at threshold. This finding confirms similar conclusions derived from studies using the trapped-electron method.[41,50]

The next structures (band "*a*") form a very well-

TABLE VIII. Band "a" in N_2 (9–11 eV).

Vibrational quantum number	Energy of[a] minimum in derivative (eV)	Spacing[b] (meV)
0	9.23	
1	9.35	130
2	9.49	125
3	9.61	120
4	9.73	120
5	9.85	115
6	9.96	115
7	10.07	110
8	10.18	105
9	10.29	105
10	10.39	100
11	10.49	100
12	10.58	90
13	10.67	90
14	10.76	90
15	10.85	85
16	10.93	85
17	11.02	85

[a]Absolute error of the energy ± 0.05 eV. Relative error ± 0.003 eV.

[b]The spacings are given to the nearest 5 meV.

developed progression of 18 vibrational levels which extends from 9 to 11 eV. The energy of each structure and the corresponding spacings are given in Table VIII. We have attempted to correlate the energies of this progression with vibrational energy levels of the known states[26] in this energy region, namely, the $B'\,^3\Sigma_u^-$, $a\,^1\Sigma_u^-$, $a\,^1\Pi_g$, and $W^3\Delta_u$ valence excited states. None of these states nor any combination of them could reproduce the spacing of band "a".

The energetically lowest Rydberg negative-ion state of N_2^- has been identified as a $^2\Sigma_g^+$ state lying at 11.49 eV. Hence band "a" cannot be associated with a parent Rydberg state. We are left with two possible explanations for the existence of band "a": (i) The band results from sharp thresholds for vibrational excitation of an unknown valence state or (ii) the band results from the formation of a N_2^- state whose parent would have to be a valence state.

TABLE IX. Features in CO (10–15 eV).

Feature number	Transmission (Present work)	Differential (Ref. 52)	
		$v=0$	$v=1$
1–1′	9.98–10.04	10.02	10.02
2–2′	10.24–10.29		10.28
3	10.42	10.38	10.46
4–4′	10.65–10.72	10.80	
5	11.27		
6	12.17		

This latter suggestion contradicts the theory of Weiss and Krauss[51] which has been proven to be correct for all other core-excited resonances we observe in N_2, CO, O_2, and NO. On the other hand, it is extremely unlikely[26] that an extensive unknown band system exists in the 9–11-eV range. This remarkably regular progression bears further investigation.

VIII. RESULTS IN CO

The electron configurations and the resulting negative-ion electronic energy levels of diatomic molecules are determined essentially by the number of electrons and should therefore be very similar for the isoelectronic molecules N_2 and CO. The electron transmission spectrum of CO is shown in Fig. 12 where the most dominant structures are labeled (1-1′) to 6. The location of each structure is given in Table IX and compared with the data of Comer and Read.[52]

Structures (1-1′) to (4-4′)

Structures (1-1′) to (4-4′) in the derivative transmission spectrum of CO, shown in Fig. 12 exhibit a remarkable resemblance with the structures (1-1′) to (4-4′) in N_2 and can be interpreted similarly. The parents of all four resonances are the

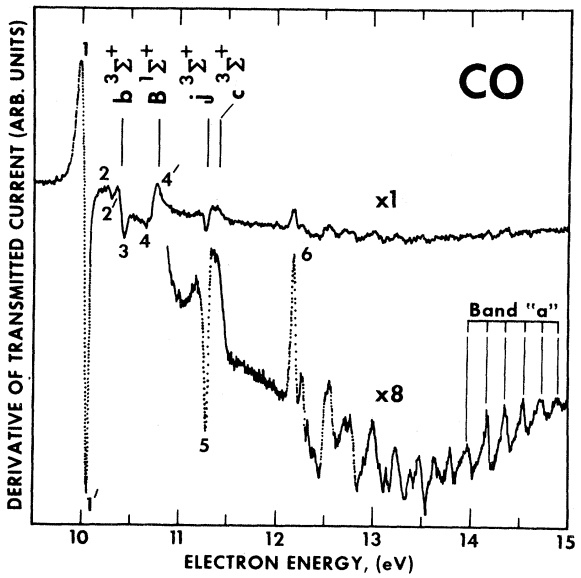

FIG. 12. Derivative of transmitted current vs electron energy in CO. Resonances 1–4 are associated with the $b\,^3\Sigma^+$ and $B\,^1\Sigma^+$ parent states of CO. The locations of these states and the j and c states are indicated. Band "a" whose grandparent is the $A\,^2\Pi$ state of CO^+, appears near the end of the spectrum. The gain on the lower curve has been increased by a factor of 8. The smaller structures on that curve represent variations in the transmitted current of about 0.01% which is the detection limit of the present experiment.

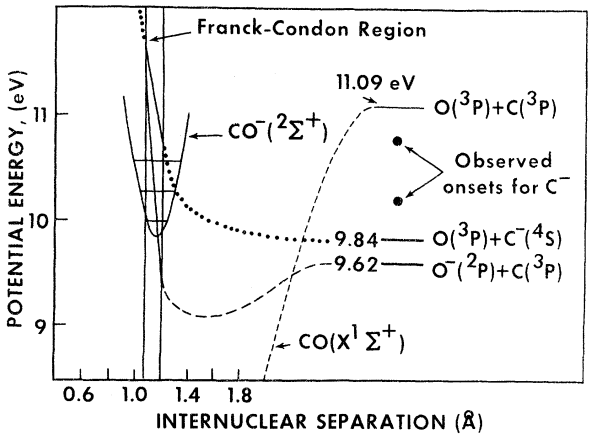

FIG. 13. Hypothetical potential-energy curves for CO^- systems showing the possible decay of the $^2\Sigma^+$ resonance at 10 eV into the $O^-(^2P)+C(^3P)$ and $O(^3P)+C^-(^4S)$ dissociative attachment channels. The vertical lines indicate the Franck-Condon region. Outside this region the shape of each potential-energy curve is uncertain and has not necessarily been drawn to scale. The onsets for the negative ions are taken from the work of Stamatovic and Schulz.

$b\,^3\Sigma^+$ and $B\,^1\Sigma^+$ states of CO while the grandparent is the $X\,^2\Sigma^+$ ground state of CO^+.

The resonance (1-1′) at 10.04 ± 0.03 eV has been confirmed and analyzed in greater detail by other authors[45,52,53] using different methods of observation. General agreement between different experiments[52,54,55] exists regarding the natural width of this resonance (45 meV). Angular distribution measurements show that the 10-eV resonance exhibits itself in the s wave,[53] thus suggesting a $^2\Sigma^+$ symmetry for this negative-ion state.

The parent $b\,^3\Sigma^+$ and $B\,^1\Sigma^+$ states show a resonant structure at threshold in differential inelastic cross-section measurements.[45]

The fact that a resonance exists at 10 eV in CO provides a simple interpretation of the results obtained by Stamatovic and Schulz[56] on O^- and C^- production by dissociative attachment of electrons in CO. A hypothetical energy-level diagram proposed to explain their results is shown in Fig. 13. These authors measured the onset for O^- formation to be 9.65 eV, in agreement with the dissociation energy of $O^-(^2P)+C(^3P)$. The lowest potential-energy curve in Fig. 13 accounts for these results. They also observed a structure at 10 eV in the cross section for O^- production. We suggest that the structure they observed results from partial decay of the 10.04 resonance into the dissociative attachment channel. It can be seen from Fig. 13 that the $^2\Sigma^+$ state of CO^- which supports the 10-eV resonance crosses the potential-energy curve leading to O^- formation in the Franck-Condon region. Thus interference from the $^2\Sigma^+$ compound state causes structure in the O^- production cross section.

Stamatovic and Schulz[56] observed two onsets for C^- production from CO at 10.2 and 10.8 eV with a small structure around 10.5 eV. The first onset is delayed by 0.36 eV with respect to the $O(^3P)+C^-(^4S)$ dissociation limit which lies 9.84 eV above the ground state of CO. Figure 13 is drawn such that the repulsive potential-energy curve leading to $C^-(^4S)+O(^3P)$ crosses the curve representing the $^2\Sigma^+$ compound state near 10.2 eV. If these two curves strongly interact, C^- formation becomes possible above 10.2 eV but only via the $^2\Sigma^+$ CO^- state. At higher energies, C^- formation is possible directly through the repulsive curve when it crosses the Franck-Condon region and a second onset is observed at 10.8 eV.

Although compound-state formation is expected to be similar in the isoelectronic molecules N_2 and CO, the $^2\Sigma^+$ resonance in CO has a natural width ($\Gamma \simeq 50$ meV) which is almost two orders of magnitude greater than the one found[40] for the $^2\Sigma_g^+$ resonance at 11.49 eV in N_2 ($\Gamma \simeq 0.6$ meV). The larger width in CO probably results from the partial decay of the $^2\Sigma^+$ resonance into the $O^-(^2P)+C(^3P)$ channel. In N_2 dissociative attachment is not observed, and the potential-energy curve corresponding to the one leading to O^-+C in CO could occur at a different energy where it would not interact with the $^2\Sigma_g^+$ state of N_2^-. Thus the natural width of the $^2\Sigma_g^+$ state in N_2^- would be small since this state decays almost exclusively[45] to the ground state of the molecule.

Band "a"

At higher energies in CO we observe many overlapping resonances, and identification of particular bands is not possible. We were able, however, to identify six vibrational levels belonging to a common progression (band "a") near the end of the spectrum shown in Fig. 12. This progression starts at 13.95 ± 0.05 eV with a spacing of 205, 190, 185, 175, and 165 ± 5 meV, respectively. The probable grandparent is the $A\,^2\Pi$ state of CO^+.

It should be noted that we do not observe a progression of resonances below 10.04 eV, i.e., below the first core-excited resonance. Thus the mysterious band "a" in N_2, which terminates near the first core-excited resonance (11.49 eV) does not seem to have an analog in CO.

IX. CONCLUSIONS

We have shown in this paper that in N_2, CO, O_2, and NO a sharp core-excited resonance always exists 0.4–0.5 eV below the lowest Rydberg state ($3s\sigma$) of the respective molecule.

In CO, O_2, and NO all the sharp resonances have Rydberg excited states as parents. Thus we confirm for these gases the theoretical consideration of Weiss and Krauss[9] who point out that Rydberg

states, but not valence states, are expected to have sharp resonances associated with them. In N_2, a mysterious band (9–11 eV) seems to be associated with a valence excited state of the neutral system. With the exception of the latter, we interpret the negative-ion states observed in the present experiment as consisting of two Rydberg electrons bound by the field of a singly charged molecular ion which we call the grandparent. The binding energy of the two $3s\sigma$ electrons to any positive-ion core always seems to be 4.2 ± 0.2 eV, regardless of the core. The internuclear parameters of the grandparent are not appreciably altered by the presence of the two Rydberg electrons. The appropriate grandparent ion state can be identified by comparing its vibrational spacings and Franck-Condon probabilities with the corresponding parameters for the observed negative-ion band.

In N_2 and CO we postulate the presence of two core-excited shape resonances which appear slightly above the first Rydberg state of the respective molecule.

ACKNOWLEDGMENTS

The authors wish to express their appreciation for valuable discussions with A. Herzenberg and P. D. Burrow. We would also like to acknowledge our indebtedness to A. L. Smith for his valuable comments and suggestions on important points related to spectroscopic data. We are grateful to F. Read and to H. S. Taylor for their comments on the paper.

---

*Work supported by the U. S. National Science Foundation.

[1]For a review, see H. S. W. Massey and E. H. S. Burhop, *Electronic and Ionic Impact Phenomena* (Clarendon, Oxford, 1969), Vol. I.

[2]For a review, see H. S. W. Massey and E. H. S. Burhop, in Ref. 1, Vol. II.

[3]J. N. Bardsley and F. Mandl, Rep. Progr. Phys. 31, 471 (1968).

[4]L. Sanche and G. J. Schulz, Phys. Rev. A 5, 1672 (1972).

[5]H. S. Taylor, G. V. Nazaroff, and A. Golebiewski, J. Chem. Phys. 45, 2872 (1966).

[6]A. Herzenberg, J. Chem. Phys. 51, 4942 (1969).

[7]G. J. Schulz and R. K. Asundi, Phys. Rev. 158, 25 (1967).

[8]H. Ehrhardt, L. Langhans, and F. Linder, Z. Physik 214, 179 (1968).

[9]A. W. Weiss and M. Krauss, J. Chem. Phys. 52, 4363 (1970).

[10]A. Stamatovic and G. J. Schulz, Rev. Sci. Instr. 39, 1752 (1968); 41, 423 (1970).

[11]C. E. Kuyatt, S. R. Mielczarek, and J. A. Simpson, Phys. Rev. Letters 12, 293 (1964).

[12]C. E. Kuyatt, J. A. Simpson, and S. R. Mielczarek, J. Chem. Phys. 44, 437 (1966).

[13]H. G. M. Heideman, C. E. Kuyatt, and G. E. Chamberlain, J. Chem. Phys. 44, 440 (1966).

[14]M. G. Menendez and H. K. Holt, J. Chem. Phys. 45, 2743 (1966).

[15]A. Weingartshofer, H. Ehrhardt, V. Herman, and F. Linder, Phys. Rev. A 2, 294 (1970).

[16]H. S. Taylor and J. K. Williams, J. Chem. Phys. 42, 4063 (1965).

[17]I. Eliezer, H. S. Taylor, and J. K. Williams, J. Chem. Phys. 47, 2165 (1967).

[18]J. Comer and F. H. Read, J. Phys. B 4, 368 (1971).

[19]J. W. McGowan and J. F. Williams, in *Abstracts of the Sixth International Conference on Physics of Electronic and Atomic Collision* (MIT Press, Cambridge, Massachusetts, 1969), p. 506.

[20]F. M. J. Pichanick, S. A. Lawton, and R. D. Dubois, in *Abstracts of the Seventh International Conference on the Physics of Electronic and Atomic Collisions, Amsterdam*, 1971 (North-Holland, Amsterdam, 1971), p. 339.

[21]J. T. Dowell and T. E. Sharp, Phys. Rev. 167, 124 (1968).

[22]K. F. Black and N. F. Lane, in Ref. 20, p. 332.

[23]H. Ehrhardt and A. Weingartshofer, Z. Physik 226, 33 (1969).

[24]D. E. Golden, Phys. Rev. Letters 27, 227 (1971).

[25]L. Sanche and G. J. Schulz, Phys. Rev. Letters 26, 943 (1971).

[26]G. Herzberg, *The Spectra of Diatomic Molecules* (Van Nostrand, Princeton, N. J., 1967); for the newest values, see B. Rosen, *Spectroscopic Data Relative to Diatomic Molecules* (Pergamon, New York, 1970).

[27]R. W. Nicholls, J. Phys. B 1, 1192 (1968); see also R. K. Asundi and Ch. V. S. Ramachandrarao, Chem. Phys. Letters 4, 89 (1969).

[28]M. E. Wacks, J. Chem. Phys. 41, 930 (1964).

[29]F. H. Mies, Phys. Rev. 175, 164 (1968).

[30]L. Sanche and G. J. Schulz, Phys. Rev. Letters 27, 1333 (1971).

[31]T. Betts and V. McKoy, J. Chem. Phys. 54, 113 (1971).

[32]E. Miescher, Helv. Phys. Acta 29, 135 (1956).

[33]The A state has been observed in electron impact spectroscopy by E. N. Lassetre, A. Skerbele, M. A. Dillon, and K. J. Ross, J. Chem. Phys. 48, 5066 (1968).

[34]C. Paquet, P. Marchand, and P. Marmet, Can. J. Phys. 49, 2013 (1971).

[35]O. Edqvist, E. Lindholm, L. E. Selin, H. Sjögren, and L. Asbrink, Arkiv Fysik 40, 439 (1970).

[36]The Franck-Condon factors for vibrational excitation of the $B\,^1\Pi$ and the $c\,^3\Pi$ state are expected to be of the same order of magnitude.

[37]J. A. R. Samson, Phys. Letters 28A, 391 (1968).

[38]It should be noted that dips which occur in the derivative transmission curve, like those observed at 12.73 and 12.94 eV, can be, *a priori*, interpreted as sharp inelastic onsets. However, it is our experience that sharp onsets in our experiment are usually associated with compound-state formation. For example, a sharp inelastic onset is often the produce of the decay of a nearby resonance when the new inelastic channel opens up. This fact influences our interpretation of the 12.73- and 12.94-eV structures as resonances.

[39]P. G. Burke, J. W. Cooper, and S. Ormonde, Phys. Rev. 183, 245 (1969).

[40]J. Comer and F. H. Read, J. Phys. B 4, 1055 (1971).
[41]R. I. Hall, J. Mazeau, J. Reinhardt, and C. Schermann, J. Phys. B 3, 991 (1970).
[42]H. G. M. Heideman, C. E. Kuyatt, and G. E. Chamberlain, J. Chem. Phys. 44, 355 (1966).
[43]R. W. Nicholls, J. Res. Natl. Bur. Std. (U.S.) 65A, 451 (1961).
[44]M. Ogawa and Y. Tanaka, Can. J. Phys. 40, 1593 (1962).
[45]N. Swanson, J. W. Cooper, and C. E. Kuyatt, in Ref. 20, p. 344.
[46]H. Ehrhardt and K. Willmann, Z. Physik 204, 462 (1967).
[47]W. L. Borst and E. C. Zipf, Phys. Rev. A 3, 979 (1971).
[48]R. Clampitt and A. S. Newton, J. Chem. Phys. 50, 1967 (1969).
[49]J. Olmsted, A. S. Newton, and K. Street, J. Chem. Phys. 42, 2321 (1965).
[50]H. H. Brongersma, A. J. H. Boerboom, and J. Kistemaker, Physica 44, 449 (1969); see also, H. H. Brongersma and L. J. Oosterhoff, Chem. Phys. Letters 1, 169 (1967).
[51]Weiss and Krauss (Ref. 9) postulate that only Rydberg excited states in molecules possess a positive electron affinity, and therefore sharp core-excited resonances are only expected energetically below Rydberg states. However a valence excited state could support a core-excited shape resonance under very favorable conditions where the capture electron would possess a high angular momentum. Such a resonant process could give rise to sharp structure.
[52]J. Comer and F. H. Read, J. Phys. B 4, 1678 (1971).
[53]L. Sanche, Z. Pavlovic, M. J. W. Boness, and G. J. Schulz, in Ref. 20, p. 350; see also, J. Comer and F. H. Read, in Ref. 20, p. 342.
[54]By fitting the derivative of a resonance line shape, as given by the Fano formula, to our data, we obtain a value of 49 ± 5 meV for the width of this resonance.
[55]Z. Pavlovic, M. J. W. Boness, and G. J. Schulz (unpublished).
[56]A. Stamatovic and G. J. Schulz, J. Chem. Phys. 53, 2663 (1970).

PHYSICAL REVIEW A VOLUME 6, NUMBER 1 JULY 1972

Relative Energies of the Lowest Levels of the $f^q ps^2$, $f^q ds^2$, and $f^{q+1} s^2$ Electron Configurations of the Lanthanide and Actinide Neutral Atoms*

K. L. Vander Sluis and L. J. Nugent
Transuranium Research Laboratory, Oak Ridge National Laboratory, Oak Ridge, Tennessee 37830
(Received 27 August 1971; revised manuscript received 6 March 1972)

Linearization of the differences between the lowest levels of the $f^q ps^2$, $f^q ds^2$, and $f^{q+1} s^2$ electron configurations as a function of q is demonstrated for the lanthanide and actinide series. A linear extrapolation of these differences estimates the energy of the lowest level of the $4f^{14}6p6s^2$ electron configuration of Lu to be 3.5×10^3 cm^{-1} higher than the measured value. This deviation from linearity is attributed to expected discontinuities at the $q=0$ and 14 ends of the $f^q ds^2$ series. In the actinide series the corresponding linear extrapolation predicts the lowest level of the $5f^{14}7p7s^2$ electron configuration of Lr to be $(2.3 \pm 3) \times 10^3$ cm^{-1} above the expected $5f^{14}6d7s^2$ ground state, after correction for a corresponding 3.3×10^3 cm^{-1} deviation expected at the end of the actinide series.

Rapidly accumulating spectroscopic data for the members of the lanthanide (Ln) and actinide (An) series have yielded important new information on the relative energies of the lowest levels of the principal electron configurations. As a result there have been a number of recent efforts to correlate and predict these relative energies.[1-6] Our approach is based on the simple yet surprisingly accurate assumption that the distinctive irregular characteristic in the energy differences

$$E(f^q ls^2) - E(f^{q+1} s^2) \equiv \Delta_l E(q) \qquad (1)$$

between the lowest levels of the indicated electron configurations involve only the electrostatic and spin-orbit interaction energies of the parent f^q and f^{q+1} configurations. Examples of this distinctive irregular characteristic are found here in Figs. 1–4, where the $\Delta_l E(q)$ are plotted for $l=p$ and $l=d$, for both the $4f$ (Ln) and $5f$ (An) series elements. The residual regular contributions to these energy differences derive primarily from electron attraction by the effective nuclear charge and from repulsions between the f electrons and the outer valence s^2, p, and d electrons. These we treat to a good approximation as linear in q, the number of f electrons in the parent f^q configuration, where q goes from 0 to 13 across each series.

Previously[1] we applied Jørgensen's expression[7]

$$\Delta_l E(q) = W + (E - A)\, q - \tfrac{9}{104} N(S) E^1 - M(L) E^3 - P(S, L, J)\, \zeta_f \qquad (2)$$

(which derives from an extension of Griffith's treatment[8] of the third ionization potentials of the first transition series) in a successful correlation of $\Delta_d E(q)$ for the neutral gaseous atoms of the Ln